Cisplatin induces acute kidney injury and pyroptosis in mice through the exosome miR-122/ELAVL1 regulatory axis

Bei Zhu
The First Affiliated Hospital of Nanjing Medical University
Xiaoshuang Ye
Jiangsu Geriatric Hospital
Fei Gao
The First Affiliated Hospital of Nanjing Medical University
Yun Bai
Nanjing First Hospital of Medical University
Zhouyi Chan
The First Affiliated Hospital of Nanjing Medical University
Lulu Guo
The First Affiliated Hospital of Nanjing Medical University
Xiaohua Pei
The First Affiliated Hospital of Nanjing Medical University
Zhenzhu Yong
The First Affiliated Hospital of Nanjing Medical University
Weihong Zhao (zhaoweihongny@njmu.edu.cn)
The First Affiliated Hospital of Nanjing Medical University

Research

Keywords: cisplatin, Acute kidney injury (AKI), pyroptosis, miR-122, ELAVL1

Posted Date: July 16th, 2020

DOI: https://doi.org/10.21203/rs.3.rs-41893/v1

Abstract

Background

Although cisplatin is an effective chemotherapeutic drug for the treatment of various cancers, its clinical application is limited due to its side effects, especially nephrotoxicity. Unfortunately, Acute kidney injury (AKI) caused by cisplatin remains one of the main obstacles to cancer treatment. Increasing evidence suggests that renal inflammation and pyroptotic inflammatory cell death of tubular epithelial cells (RTECs) mainly determine the progression and outcome of cisplatin-induced AKI. However, it is not clear how cisplatin regulates the pyroptosis of RTECs cells in AKI. The current study aimed to determine the regulation mechanism of AKI induced by cisplatin. In vivo, cisplatin was used to induce AKI. H&E staining of mouse kidney tissue sections and serological indicators of kidney injury (including BUN, serum creatinine and TNF-α) were detected. The important substrate protein GSDMD and key target caspase-1 of pyroptosis were detected by immunohistochemistry and western blot, respectively. In vitro, cisplatin significantly induces HK-2 cells pyroptosis. Furthermore, Cisplatin transmits HK2 cells pyroptosis signals to surrounding cells in the form of exosomes. Previous studies have shown that exosomes are involved in kidney physiology and the pathogenesis of various kidney diseases/disorders. MicroRNAs (miRNAs) are the main functional components of exosomes.

Results

Further research shows that exosome miR-122 negatively regulates the pyrolysis of HK2 cells. Finally, we elucidated that exosome miR-122 participates in cisplatin induced AKI regulation by regulating ELAVL1 expression.

Conclusions

In conclusion, these results suggest that exosome miR-122 inhibits pyroptosis and AKI by targeting ELAVL1 under cisplatin treatment, which will provide a potential target for the treatment of AKI.

Introduction

Cisplatin is a heavy metal compound with a widely clinical application in various tumors. It is one of the most extensive, effective and valuable adjuvant chemotherapy drugs for treating diverse malignant tumors, including ovarian cancer, cervical cancer and so on [1]. Regardless of its potential medicinal effects, nephrotoxicity caused by cisplatin is one of the main factors limiting its clinical application [2]. Approximately one-third of patients treated with cisplatin suffered from renal dysfunction and injury, especially acute kidney injury (AKI), which has become the most difficult problem in the application of cisplatin [3]. Unfortunately, there is currently no effective treatment to prevent cisplatin-induced AKI [4]. Therefore, it is of great significance to explore the regulation mechanism of cisplatin-induced AKI.

AKI is characterized by a sudden decrease in renal function, manifested by an increase in serum creatinine ≥ 0.3 mg/dL or a decrease in urine output of 0.5 mL/kg/h, and is closely related to high morbidity and mortality [5]. The mechanisms of cisplatin-induced AKI are complex, mainly manifested as excessive inflammation and programmed cell death of renal tubular epithelial cells (RTECs) [6]. In the kidney, RTECs are the main target of drug-induced nephrotoxicity and are particularly vulnerable to cisplatin injury [7]. Previous studies have also shown that the common histological feature of cisplatin-induced AKI is renal damage caused by renal tubular cell death [8].

Pyroptosis is a new type of proinflammatory programmed cell death regulated by caspases discovered and confirmed in recent years. Its morphological feature is the formation of plasma membrane pores, leading to the secretion of intracellular components and inflammatory cytokines [9]. Early research first observed the phenomenon of pyroptosis in several phagocytes, such as macrophages [10]. However, recent studies have found that pyroptosis can also be triggered in other types of cells, such as RTECs [11]. A growing number of studies have focused on the role of pyroptosis in AKI. Caspase-11-mediated pyroptosis of RTECs promotes acute renal injury induced by septic [12]. The TNF-α/HMGB1 inflammation signal axis participates in the progression of AKI disease by regulating pyroptosis [13]. Acetylbritannilactone can alleviate contrast-induced AKI by reducing pyroptosis [14]. Furthermore, increasing evidences indicate that RTECs pyroptosis and renal inflammation are involved in the regulation of cisplatin-induced AKI progression and outcome. For example, the cleavage of GSDMD by caspase-11 may promotes cisplatin-induced AKI by triggering RTECs pyroptosis [15]. These studies indicate that the pyroptosis of RTECs is a key event in the occurrence and outcome of cisplatin-induced AKI. However, the exact mechanism by which cisplatin induces AKI by promoting pyroptosis is unclear.

Exosomes are microvesicles of multivesicular bodies with diameters ranging from 20 to 200 nm [16]. Exosomes participate in cell-to-cell communication with recipient cells by fusing with receptor cell membranes and delivering biomolecules such as proteins, DNA, mRNAs and miRNAs [17]. In recent years, more and more studies have revealed the function of exosomes in the kidney. On the one hand, exosomes can be used as a marker for early diagnosis and treatment of kidney disease [18]; On the other hand, exosomes target effector cells through the paracrine pathway to play a role in kidney pathophysiology [19]. Previous study found that injured renal tubular epithelial cells activate fibroblasts through exosome miRNAs to promote renal fibrosis [20]. Limb remote ischemic preconditioning induces systemic up-regulation of exo-miR-21, exerting anti-inflammatory and anti-apoptotic effects, thereby protecting sepsis-induced AKI [21]. However, the regulatory mechanism of exosomal miRNAs in cisplatin induced AKI is unclear.

To investigate whether exosomal miRNAs plays a role in cisplatin-induced AKI by regulating pyroptosis, we first used cisplatin to induce AKI mouse model. Then, we analyzed the expression of GSDMD, a key substrate protein for pyroptosis, in AKI mice by immunohistochemistry (IHC). We also detected the expression of pyroptosis-related proteins caspase-1 and GSDMD-N by Western blot (WB) analysis. The results showed that pyroptosis occurred when cisplatin induced AKI in mice. Next, we studied in vitro. We treated HK2 cell line with cisplatin and detected the expression of caspase-1 by immunofluorescence (IF).

We also measured the expression of GSDMD-N in HK2 cell line by WB. The experimental results are consistent with animal levels. Therefore, we further studied the regulatory mechanism of cisplatin induced AKI. When we added cisplatin and GW4869 at the same time, the expression of caspase-1, NLRP3 and GSDMD was significantly down-regulated. These results indicate that cisplatin regulates HK2 cell pyroptosis through exosomes. Further in vitro and in vivo, the gain- or loss- of function experiments were done to clarify that cisplatin affects pyroptosis of RTECs through the exosomal miR-122/ELAVL1 regulatory axis in cisplatin induced AKI.

Materials And Methods

Cell lines and culture conditions

HK2 cells (human renal tubular epithelial cells) were purchased from the Chinese Academy of Sciences, Shanghai Institute of Biochemistry and Cell Biology (Shanghai, China). These cells were grown in DMEM containing 5% FBS (37 °C, 5% CO_2). The HK2 cells were treated with or without 20 μM cisplatin for 24 h.

Animal model of AKI

Adult male C57BL/6 mice (8–12 weeks of age) were obtained from Model Animal Research Center of Nanjing University, Nanjing, China. All animal procedures have been approved by the Institutional Animal Experimental Ethics Committee. 20 mg/kg cisplatin was injected. Cisplatin-induced AKI mice model was constructed as described previously [22]. These mice were intraperitoneally injected with 20 mg/kg body weight cisplatin, and equal volume of 0.9% saline were injected as controls. After 72 hours, the mice were killed under anesthesia. We collected blood samples and kidney tissues for further study.

Serum Creatinine, BUN, TNF-α and Histology

We used a Beckman creatinine analyzer II (DXC800; Beckman Coulter) to analyze the serum creatinine concentration in model mice. BUN was measured using a BUN Assay Kit (Nanjing, China) according to the manufacturer's instructions. The TNF-α levels were detected using the TNF-α Assay Kit (Nanjing, China) according to the manufacturer's instructions. A 2 μm-thick section was used for hematoxylin-eosin staining (H&E) to assess renal tubular histological damage.

Immunohistochemistry

Paraffin-embedded renal tissue sections in AKI mice were used to detect the expression of GSDMD (ab219800; 1:1000; Abcam, UK), a marker of pyroptosis, by immunohistochemistry (IHC). The specific experimental procedures of IHC refer to previous reports [23].

Immunofluorescence staining

The HK2 cells were placed on glass slides in 6-well plates. After cisplatin treatment for 24 h, the cells were fixed in 4% paraformaldehyde, blocked with 2% BSA and incubated with 0.1% Triton X-100. The HK2 cells were incubated with caspase-1 antibody (sc-398715, Santa Cruz Biotechnology, 1:200, USA) at 4 °C

overnight. The slides were subsequently incubated with secondary antibody (Alexa Fluor 488-labelled). The nuclei were stained using DAPI. The specific experimental procedures of IHC refer to previous reports [24].

RNA extraction and qRT-PCR

The extraction of total RNA and the analysis of qRT-PCR were performed according to the previous description [1]. We used TRIZOL reagent (Thermofisher, USA) to extract total RNA by in cells and tissues. Taqman probes (Applied Biosystems, USA) were used to quantify miRNAs. Briefly, 1 μg of total RNA was transcribed to cDNA using AMV reverse transcriptase (Takara, Japan) and a RT primer. The reaction conditions were: 16 °C for 30 min, 42 °C for 30 min and 85 °C for 5 min. Real-time PCR was performed using a Taqman PCR kit on an Applied Biosystems 7300 sequence detection system (Applied Biosystems, USA). The reactions were performed in a 96-well plate at 95 °C for 10 min, followed by 40 cycles of 95 °C for 10 sec and 60 °C for 1 min. U6 was used as the internal control. Primers: Caspase-1 FP 5′-CGGAATTCACCATGGCCGACAAGGTCCTG – 3′, RP 5′-CTGCACTGCCTGAGGAGCTGGAAAGGAAGAAAGTACTCCTTGAGAGTCT – 3′; NLRP3 FP 5′-CTCAGCCTTGCGAAGTTTCA-3′, RP 5′-ACCGCATACACACTTGGAGA-3′; GSDMD FP 5′-CTCAGCCTTGCGAAGTTTCA-3′, RP 5′-ACCGCATACACACTTGGAGA-3′; ELAVL1 FP 5′-CTCAGCCTTGCGAAGTTTCA-3′, RP 5′-ACCGCATACACACTTGGAGA-3′;GAPDH FP 5′-CTCAGCCTTGCGAAGTTTCA-3′, RP 5′-ACCGCATACACACTTGGAGA-3′; Stem loop primer FP 5′-GTCGTATCCAGTGCAGGGTCCGAGGTATT-3′, RP 5′-CGCACTGGATACGACACACCC-3′. U6 FP 5′-CTCGCTTCGGCAGCACA-3′; RP: 5′-AACGCTTCACGAATTTGCGT – 3′.

Exosome isolation and labeling

Exosome-depleted FBS was used in the following experiments to avoid the impact of exosomes. FBS was depleted of exosomes by ultracentrifugation at 1×10^6 g at 4 °C for 16 h (Beckman Coulter Avanti J-30I, USA). After being incubated for 48–72 h, the culture medium was harvested and exosomes were isolated by ultracentrifugation. Briefly, cell culture medium was sequentially centrifuged at 300 g for 10 min, 2,000 g for 15 min, and 12,000 g for 30 min to remove floating cells and cellular debris. These were then passed through a 0.22-μm filter. The supernatant was further ultracentrifuged at 1×10^6 g for 2 h at 4 °C, washed in phosphate-buffered saline (PBS), and submitted to a second ultracentrifugation in the same conditions. Exosomes were quantified with bicinchoninic acid (BCA) method. Exosomal protein was measured by BCA protein assay kit (Beyotime Biotechnology, Nantong, China). The final exosome pellets were used immediately.

Transmission electron microscope

Exosomes were precipitated and immediately fixed in 2.5% glutaraldehyde at 4 °C for the electron microscope observation. After fixation, specimens were processed through dehydration in gradient alcohol, and infiltrated in epoxy resin and then embedded. The ultrathin sections were stained with uranyl acetate and lead citrate, and were observed under transmission electron microscope (TEM) (JEM-1010; JEOL, Tokyo, Japan).

NanoSight tracking analysis (NTA)

Isolated exosomes were analyzed using Nanosight LM10 system (Nanosight Ltd, Navato, CA) equipped with a blue laser (405 nm). Nanoparticles were illuminated by the laser and their movement under Brownian motion was captured for 60 seconds and the video recorded was subjected to NTA using the Nanosight particle tracking software to calculate nanoparticle concentrations and size distribution.

Western blotting analysis

Protein lysates were fractionated on SDS-polyacrylamide gels and transferred to polyvinylidene fluoride (PVDF) membrane and blocked with 5% skimmed milk in Tris-buffered saline with Tween 20. The membranes were incubated with the primary antibodies, including Caspase-1 rabbit monoclonal antibody (ab207802; 1:1000; Abcam, UK), GSDMD-N rabbit monoclonal antibody (ab215203; 1:1000; Abcam, UK), NLRP3 rabbit monoclonal antibody (ab263899; 1:1000; Abcam, UK), GSDMD rabbit monoclonal antibody (ab219800; 1:1000; Abcam, UK). ELAVL1 rabbit monoclonal antibody (ab200342; 1:1000; Abcam, UK). CD63 rabbit monoclonal antibody (ab134045; 1:1000; Abcam, UK). CD9 rabbit monoclonal antibody (ab92726; 1:2000; Abcam, UK). The protein concentration of the supernatant was determined with a BCA protein assay kit (synthgene, China). GAPDH served as a loading control and protein bands were quantified using Image J Software.

Luciferase reporter assay

pMIR-ELAVL1-3'-UTR-WT as well as pMIR- ELAVL1-3'-UTR-MUT luciferase reporter plasmids were constructed by Synthgene Biotech (Nanjing, China). The sequences that could binding to miR-122 were partly mutated and inserted into the reporter plasmid in order to identify the binding specificity. The implementation method refers to previous study [25]. Briefly, HK2 cells were seeded in a 24 well plate until reaching 60% confluence. Each well was co-transfected with luciferase reporter plasmids (0.5 μg) and RNA mimics (100 pmol) using Lipofectamine 2000 (Thermofisher, USA) according to the manufacturer's protocol. The luciferase activity was measured after 48 h of transfection, by using the Dual-Luciferase Reporter Assay (Promega, Shanghai, China) according to the manufacturer's instructions and normalized to Renilla signals.

siRNA preparation and transfection

ELAVL1 knockdown was accomplished by transfecting cells with siRNA. ELAVL1 and control siRNA were synthesized by Synthgene (China). The specific method refers to the previous description [25]. The sequences were as follows: the ELAVL1 sense GAACATGACCCAGGATGAGTT, the ELAVL1 antisense UUUUGAAGAAGAAUCGUUGcc. SiRNA transfection into HK2 cells was carried out using Lipofectamine 2000 (Thermofisher, USA) according to the manufacture’s instruction.

Overexpression plasmid construction

Full-length ELAVL1 from the human cDNA library was cloned into a pcDNA3.1 vector (Invitrogen; Thermo Fisher Scientific, Inc.). The pcDNA3.1 vector alone (empty plasmid) served as a negative control. HK2

cells were transfected with pcDNA3.1/ ELAVL1 vector (100 nM) or pcDNA3.1 (100 nM) using Lipofectamine 2000 (Thermofisher, USA) according to the manufacture's instruction. Following transfection for 48 h, the cells were collected for subsequent experiments. The sequence of the ELAVL1 overexpressed plasmid is detailed in the supplementary materials.

Statistical analyses

All experiments were repeated three times and the data are presented as the mean ± standard deviation using SPSS 18.0 (SPSS, inc.). One-way ANOVA and post hoc Dunnett's T3 test were performed in order to compare the differences among and between groups, respectively. $P < 0.05$ was considered to indicate a statistically signifcant result.

Results

Cisplatin induces mouse AKI and RTECs pyroptosis.

Cisplatin-induced AKI seriously threatens the health of cancer patients and largely limits its application to chemotherapy [26]. Therefore, it is of great significance to study the pathogenesis of cisplatin-induced AKI. First, we constructed an AKI mouse model by cisplatin induction. We then detected histopathological damage to the renal cortex of cisplatin-induced AKI mice by H&E staining. As shown in Fig. 1A, cisplatin causes a moderate renal tubular injury. The kidney section showed obvious focal tubular epithelial cells swelling, dilation and detachment with moderate tubular vacuole. In addition, the levels of blood urea nitrogen (BUN) (Fig. 1B), serum creatinine (Fig. 1C) and TNF-α (Fig. 1D) were significantly increased in cisplatin-AKI mice model.

Previous study found that pyroptosis plays an important role in many inflammatory diseases, such as cisplatin-induced AKI [23]. Therefore, in this study we further explored how pyroptosis participates in cisplatin-induced AKI. First, we detected the expression of GSDMD in kidney tissue by IHC analysis. As shown in Fig. 1E, the expression of GSDMD in the model group (cp) was significantly increased when compared with the control group. Then, we detected the expression levels of caspase-1 and GSDMD-N by WB analysis. The variation trend of the results is consistent with GSDMD (Fig. 1F-G). These in vivo experiments preliminarily elucidated the involvement of pyroptosis in cisplatin-induced AKI.

In order to further elucidate the role of pyroptosis in cisplatin-induced AKI, we conducted further studies in vitro. HK2 cell lines (human RTECs) were selected for the study. First, the expression of caspase-1 in HK2 cells were detected by IF when treated with cisplatin. As shown in Fig. 1H, the expression level of caspase-1 in HK2 cells treated with cisplatin was significantly increased when compared with the control group. Then, we detected the expression level of GSDMD-N in HK2 cells when treated with cisplatin. The variation trend of the results is consistent with caspase-1 (Fig. 1I-J). In summary, these in vivo and in vitro results indicate that pyroptosis is involved in cisplatin-induced AKI.

HK2 cell-derived exosomes treated with cisplatin influenced pyroptosis of surrounding HK2 cells.

Previous studies have reported that exosomes play a key role in the development of kidney disease. However, there are few reports on cisplatin-induced AKI, and the regulatory mechanism is unclear. Therefore, in the present study, we explored the role of exosomes in cisplatin-induced pyroptosis of HK2 cells. First, HK2 cells were treated with cisplatin and exosome inhibitor GW4869 at the same time, and the expression of caspase-1 was detected by IF. As shown in Fig. 2A, the treatment of HK2 cells with cisplatin can significantly increase the expression of caspase-1, but after adding GW4869, the expression of caspase-1 was significantly down-regulated. This result suggests that exosomes are involved in cisplatin-induced pyroptosis of surrounding HK2 cells. To further verify our hypothesis, we also detected the mRNA and protein expression levels of caspase-1, NLRP3 and GSDMD by qRT-PCR and WB, respectively. The variation trend of the results is consistent with caspase-1 (Fig. 2B-D). Taken together, these results indicate that exosomes are involved in cisplatin-induced AKI pyroptosis.

Next, we focused on the exosomes in HK2 cells. Therefore, we further isolated and identified exosomes from HK2 cells. As shown in Fig. 2E, exosomes were characterized by transmission electron microscope (TEM). TEM analysis of isolated exosomes showed round structures with diameters between 30 and 150 nm. The qNano analysis was used to quantify the particle diameter of the population of small vesicles collected from HK2 cells and the mean diameter of HK2-exo detected was 100 nm (Fig. 2F). We also measured exosome markers CD63 and CD63 in HK2 cells when treated with or without cisplatin. WB assay showed that CD63 and CD63 were all expressed in both ctrl-exo and cp-exo groups (Fig. 2G).

Cisplatin-treated HK2 cells exosome-derived miR-122 regulates pyroptosis in surrounding cells.

In eukaryotes, miRNAs usually regulate gene expression at the post-transcriptional level. Previous studies have found that abnormal levels of miRNA could be one of the mechanisms explaining dysregulated protein expression in the progression of kidney disease [27]. When evaluating an integrative network of miRNAs and mRNA data, miR-122 was found to be one of a possible master regulator in AKI [28]. Therefore, we speculate that miR-122 is involved in the regulation of cisplatin-induced AKI pyroptosis. To verify our hypothesis, we first tested the expression of miR-122 in AKI mice and HK2 cells. As shown in Fig. 3A-B, cisplatin treatment significantly reduced miR-122 expression in vivo and in vitro when compared with control. However, after adding GW4869, the expression of miR-122 significantly increased to close to the control group (Fig. 3C).

To further explore the role of exosomes derived miR-122 in cisplatin-induced pyroptosis of HK2 cells. First, the miR-122 mimic and inhibitor were used to transfect HK2 cells to overexpress (miR-122 OE) and knock down (miR-122 KD) miR-122, respectively. Then, the expression of caspase-1 in surrounding HK2 cells (NC) were detected by IF when adding cisplatin-treated HK2 cell-derived exosomes (cp-exo) and cisplatin-treated miR-122 OE HK2 cell-derived exosomes (cp-exo + miR-122 OE) treatments, separately. As shown in Fig. 3E, the expression level of caspase-1 was significantly increased when compared with the NC group when adding cp-exo treatment. In contrast, the expression level of caspase-1 was significantly decreased when adding cp-exo + miR-122 OE treatment. We also tested the expression of caspase-1 in miR-122KD HK2 cell line. The results showed that the expression of caspase-1 was also significantly

increased in miR-122 KD HK2 cell line when compared with the NC group. Next, we also detected the mRNA and protein expression levels of caspase-1, NLRP3 and GSDMD by qRT-PCR and WB, respectively. The variation trend of the results is consistent with caspase-1 (Fig. 3E-G). The above results further indicate that the miR-122 involved in cisplatin-treated HK2 cell exosomes affects the surrounding HK2 cell pyroptosis.

We further explored the regulatory mechanism of miR-122 involved in the regulation of pyroptosis in cisplatin-treated HK2 cells. First, the expression level of miR-122 was detected by qRT-PCR in NC, NC + cp-exo, NC + cp-exo-miR-122 OE and NC + miR-122 KD groups. As shown in Fig. 3H, the expression level of miR-122 was significantly decreased when adding cp-exo treatment. In contrast, the expression level of miR-122 was significantly increased when adding cp-exo + miR-122 OE treatment. We also tested the expression of miR-122 in miR-122KD HK2 cell line. The result was in line with expectations. Then, we predicted the relevant targets. The TargetScan Human 7.2 software was used to reveal that miR-122 targets ELAVL1. As shown in Fig. 3I, ELAVL1 gene was found to contain putative sites of the 3'-UTR untranslated region (3'-UTR) that matched to the miR-122 seed region. To investigate whether miR-122 targets ELAVL1 in cisplatin-induced AKI, we set up the luciferase reporter plasmid (containing the wild-type (WT) and mutation-type (MUT) 3'-UTR) of target gene ELAVL1 by luciferase reporter vector. We further used the transfection reagent to transfect these reporter gene plasmids (WT and MUT) into HK2 cells together with the miR-122 mimic or miR-122 inhibitor, respectively. Compared with control groups, WT reporter activity were predominantly decreased in HK2 cells when transfected with miR-122 mimic. In contrast, WT reporter activity was significantly up-regulated in HK2 transfected with miR-122 inhibitor. While, the transfection of miR-122 mimic and miR-122 inhibitor did not affect the activity of MUT reporter activity (Fig. 3J). Then, we detected the protein expression of ELAVL1 when adding cisplatin treatment in vivo and in vitro. As shown in Fig. 3K-L, the expression level of ELAVL1 was significantly increased when adding cisplatin treatment. To elucidate the role of exosomes in regulating the expression of ELAVL1. We also added GW4869 treatment. The results showed that the expression of ELAVL1 was significantly decreased in HK2 cells when adding cisplatin and GW4869 treatment at the same time (Fig. 3M).

Finally, we conducted a rescue experiment. We measured the protein expression of ELAVL1 in NC, NC + cp-exo, NC + cp-exo-miR-122 OE and NC + miR-122 KD groups. As shown in Fig. 3N, the expression level of ELAVL1 was significantly increased when adding cp-exo treatment. In contrast, the expression level of ELAVL1 was significantly decreased when adding cp-exo + miR-122 OE treatment. We also tested the expression of ELAVL1 in miR-122KD HK2 cell line. The result was in line with expectations. All these results suggest that miR-122 negatively regulates ELAVL1 expression by directly binding to the 3'-UTR region of ELAVL1 in cisplatin-induced AKI.

Exosome-derived miR-122 affects cisplatin-induced AKI and HK2 cells pyroptosis by regulating the expression of ELAVL1.

In order to further explore the role of miR-122-ELAVL1 axis in pyroptosis regulation pathway under cisplatin-induced AKI. First, we transfected the siELAVL1, miR-122 OE + ELAVL1 OE plasmid into HK2 cell

line. Then, we extracted the exosomes of these cell lines after cisplatin treatment. Exosomes derived from these cell lines were co-incubated with HK2 cells (NC) to detect the expression of caspase-1 via IF. As shown in Fig. 4A, the expression level of caspase-1 was significantly increased when adding cp-exo treatment. However, the expression level of caspase-1 was significantly decreased when adding cp-exo derived from siELAVL1 HK2 cell line treatment. In contrast, the expression level of caspase-1 was also significantly increased when adding cp-exo derived from miR-122 OE + ELAVL1 OE HK2 cell line treatment. At the same time, we detected the expression of miR-122 and ELAVL1 by qRT-PCR or WB. The experimental results were consistent with the expected results (Fig. 4B-D). Next, we also detected the mRNA and protein expression levels of caspase-1, NLRP3 and GSDMD by qRT-PCR and WB, respectively. As shown in Fig. 4E, the mRNA expression levels of caspase-1, NLRP3 and GSDMD were significantly increased when adding cp-exo treatment. However, the expression levels of caspase-1, NLRP3 and GSDMD were significantly decreased when adding cp-exo derived from siELAVL1 HK2 cell line treatment. In contrast, the expression levels of caspase-1, NLRP3 and GSDMD were also significantly increased when adding cp-exo derived from miR-122 OE + ELAVL1 OE HK2 cell line treatment. The variation trend of caspase-1, NLRP3 and GSDMD protein expression was consistent with that of mRNA (Fig. 4F). Taken together, these results indicate that the miR-122-ELAVL1 axis involved in cisplatin-treated HK2 cell exosomes affects the surrounding HK2 cell pyroptosis.

Finally, we elucidate our hypothesis in vivo. We detected histopathological damage to the renal cortex of cisplatin-induced AKI mice by H&E staining when miR-122 is overexpressed (OE) or ELAVL1 is knocked down (KD). As shown in Fig. 4G, either overexpressing miR-122 or knocking down ELAVL1 will alleviate cisplatin-induced AKI. We also detected the expression of GSDMD in kidney tissue by IHC analysis. As shown in Fig. 4H, the expression of GSDMD in the miR-122 OE and siELAVL1 AKI mice were all significantly decreased when compared with the model group. In addition, the levels of blood urea nitrogen (BUN) (Fig. 4I), serum creatinine (Fig. 4J), TNF-α (Fig. 4K), IL-1β (Fig. 4L) and IL-18 (Fig. 4M) were significantly decreased in the miR-122 OE and siELAVL1 AKI mice. We also tested the expression of miR-122 in the miR-122 OE and siELAVL1 AKI mice (Fig. 4N). At the same time, we detected the expression of ELAVL1, caspase-1, NLRP3 and GSDMD proteins in the miR-122 OE and siELAVL1 AKI mice. The results were in line with expectations (Fig. 4O). All in all, these results indicate that miR-122 inhibits cisplatin-induced AKI and HK2 cells pyroptosis via ELAVL1.

Discussion

Cisplatin is an effective chemotherapy drug and has been widely used to treat solid tumors. However, it usually causes AKI in these patients. Previous studies have found that renal insufficiency can independently predict a poor prognosis for cancer patients [29]. However, to date, the mechanism of cisplatin-induced AKI has not been studied in depth, and there is still no effective treatment. The pathological features of AKI are renal tubular cell damage, inflammation and vascular dysfunction. Among them, renal tubular cell death is a common histopathological feature of AKI, and it is generally considered to be one of the factors leading to impaired renal function [30]. Pyroptosis is a proinflammatory programmed cell death regulated by caspases, and its role in kidney damage has been

gradually discovered in recent years [9, 31]. The role of pyroptosis of RTECs in cisplatin-induced AKI has been reported [12]. In this study, we also used cisplatin induction to construct AKI mouse models, and detected the expression of GSDMD, caspase-1 and GSDMD-N, the key targets of pyroptosis by IHC and WB, respectively (Fig. 1A-G). Then the HK2 cell line was used for in vitro experiments. The results show that cisplatin treatment of HK2 cells can significantly increase the expression of caspase-1 and GSDMD-N through IF and WB, respectively (Fig. 1H-J). These results suggest that pyroptosis is involved in cisplatin-induced AKI regulation. This is consistent with previous reports. However, the regulatory mechanism is not yet clear. Therefore, studying the molecular mechanism of RTECs pyroptosis in cisplatin-induced AKI has become an exploration area for the development of new AKI therapies.

Exosomes act as an important medium of communication between cells. Exosomes participate in immune regulation, information transmission and antigen presentation [32]. Substances encapsulated in exosomes, especially miRNAs, play a vital role in the pathogenesis of various kidney diseases [33]. Exosomes derived from hBMSCs can prevent renal ischemia/reperfusion (I/R) injury through miR-199a-3p transplantation [34]. Exosome miRNA-19b-3p of RTECs promotes the activation of M1 macrophages during kidney injury [35]. However, there are few studies on exosome miRNAs in cisplatin-induced AKI, and the mechanism is not clear. In the present study, when we first added cisplatin and GW4869 to treat HK2 cells at the same time, we found that the phenomenon of pyroptosis was suppressed (Fig. 2A-D), which initially explained our hypothesis. Therefore, we further isolated and identified the exosomes of HK2 cells (Fig. 2E-G). Previous studies found that LncRNA XIST regulates the expression of ASF1A/BRWD1M/PFKFB2 through sponge adsorption of miR-212 and thus participates in the regulation of acute renal injury in renal transplantation [36]. In the present study, we measured the expression of miR-122 in AKI mice and HK2 cells when adding cisplatin treatment. As shown in Fig. 3A-B, when cisplatin was added, the expression of miR-122 was significantly down regulated. We further added GW4869 treatment and found that the expression of miR-122 was significantly restored (Fig. 3C). To verify the role of miR-122 in cisplatin-induced pyroptosis of HK2 cells. We constructed miR-122 OE and miR-122 KD cell lines. Subsequently, we added cisplatin treatment to the miR-122 OE cell line and extracted the exosomes, and incubated the exosomes with the HK2 cell line. We then tested the relevant indicators of pyroptosis. We also measured the relevant indicators of pyroptosis in miR-122 KD HK2 cell line. The results showed that miR-122 can inhibit the effect of cisplatin-treated HK2 cell exosomes on the pyroptosis of surrounding HK2 cells (Fig. 3D-G).

Next, we identified ELAVL1 as a specific target for miR-122 to regulate pyroptosis in HK2 cells (Fig. 3I). Previous studies found that MALAT1 regulates renal tubular epithelial pyroptosis by modulated miR-23c targeting of ELAVL1 in diabetic nephropathy [37]. However, the role of ELAVL1 in cisplatin-induced AKI has not been reported. In the present study, we first clarified the relationship between miR-122 and ELAVL1 through the luciferase assay (Fig. 3J). Then, we detected ELAVL1 protein expression in cisplatin-treated mice and cells. The results showed that cisplatin treatment significantly increased the expression of ELAVL1 (Fig. 3K-L). Finally, we clarified that cisplatin-treated HK2 cell exosomes affect the surrounding HK2 pyroptosis (Fig. 3M-N). Finally, we clarified miR-122 inhibits cisplatin-induced AKI and HK2 cells pyroptosis via ELAVL1 through a functional backfill experiment (Fig. 4).

In general, to our understanding, this study first described that miR-122 affects the pyroptosis of RTECs in cisplatin-induced AKI by regulating the expression of ELAVL1. This provides a new perspective for the treatment of AKI.

Declarations

Ethics approval and consent to participate

Not applicable.

Consent for publication

Not applicable.

Availability of data and materials

Not applicable.

Competing interests

The authors declared that there are no conflicts of interest.

Funding

Funding information is not applicable.

Authors' contributions

BZ and XSY designed and analyzed the experiments and were major contributors to the manuscript.The remaining authors conducted separate experiments, and all of them read and approved the final manuscript.

Acknowledgements

We would like to thank all the researchers and study participants for their contributions.

References

1. Zhang W, Chen C, Jing R, Liu T, Liu B. Remote Ischemic Preconditioning Protects Cisplatin-Induced Acute Kidney Injury through the PTEN/AKT Signaling Pathway. Oxid Med Cell Longev. 2019;2019:7629396.

2. Pabla N, Dong Z. Cisplatin nephrotoxicity: mechanisms and renoprotective strategies. Kidney Int. 2008;73(9):994–1007.
3. Dupre TV, Doll MA, Shah PP, Sharp CN, Kiefer A, Scherzer MT, Saurabh K, Saforo D, Siow D, Casson L, Arteel GE, Jenson AB, Megyesi J, Schnellmann RG, Beverly LJ, Siskind LJ. Suramin protects from cisplatin-induced acute kidney injury. Am J Physiol Renal Physiol. 2016;310(3):F248-58.
4. Crona DJ, Faso A, Nishijima TF, McGraw KA, Galsky MD, Milowsky MI. A Systematic Review of Strategies to Prevent Cisplatin-Induced Nephrotoxicity. Oncologist. 2017;22(5):609–19.
5. Holditch SJ, Brown CN, Lombardi AM, Nguyen KN, Edelstein CL. Recent Advances in Models, Mechanisms, Biomarkers, and Interventions in Cisplatin-Induced Acute Kidney Injury, Int J Mol Sci 20(12) (2019).
6. Mulay SR, Linkermann A, Anders HJ. Necroinflammation in Kidney Disease. J Am Soc Nephrol. 2016;27(1):27–39.
7. Weijl NI, Elsendoorn TJ, Lentjes EG, Hopman GD, Wipkink-Bakker A, Zwinderman AH, Cleton FJ, Osanto S. Supplementation with antioxidant micronutrients and chemotherapy-induced toxicity in cancer patients treated with cisplatin-based chemotherapy: a randomised, double-blind, placebo-controlled study. Eur J Cancer. 2004;40(11):1713–23.
8. Yang C, Guo Y, Huang TS, Zhao J, Huang XJ, Tang HX, An N, Pan Q, Xu YZ, Liu HF. Asiatic acid protects against cisplatin-induced acute kidney injury via anti-apoptosis and anti-inflammation. Biomed Pharmacother. 2018;107:1354–62.
9. Place DE, Kanneganti TD. Cell death-mediated cytokine release and its therapeutic implications. J Exp Med. 2019;216(7):1474–86.
10. Martin SJ. Cell death and inflammation: the case for IL-1 family cytokines as the canonical DAMPs of the immune system. FEBS J. 2016;283(14):2599–615.
11. Zhang Z, Shao X, Jiang N, Mou S, Gu L, Li S, Lin Q, He Y, Zhang M, Zhou W, Ni Z. Caspase-11-mediated tubular epithelial pyroptosis underlies contrast-induced acute kidney injury. Cell Death Dis. 2018;9(10):983.
12. Ye Z, Zhang L, Li R, Dong W, Liu S, Li Z, Liang H, Wang L, Shi W, Malik AB, Cheng KT, Liang X. Caspase-11 Mediates Pyroptosis of Tubular Epithelial Cells and Septic Acute Kidney Injury. Kidney Blood Press Res. 2019;44(4):465–78.
13. Wang Y, Zhang H, Chen Q, Jiao F, Shi C, Pei M, Lv J, Zhang H, Wang L, Gong Z. TNF-alpha/HMGB1 inflammation signalling pathway regulates pyroptosis during liver failure and acute kidney injury. Cell Prolif. 2020;53(6):e12829.
14. Chen F, Lu J, Yang X, Xiao B, Chen H, Pei W, Jin Y, Wang M, Li Y, Zhang J, Liu F, Gu G, Cui W. Acetylbritannilactone attenuates contrast-induced acute kidney injury through its anti-pyroptosis effects, Biosci Rep 40(2) (2020).
15. Miao N, Yin F, Xie H, Wang Y, Xu Y, Shen Y, Xu D, Yin J, Wang B, Zhou Z, Cheng Q, Chen P, Xue H, Zhou L, Liu J, Wang X, Zhang W, Lu L. The cleavage of gasdermin D by caspase-11 promotes tubular

epithelial cell pyroptosis and urinary IL-18 excretion in acute kidney injury. Kidney Int. 2019;96(5):1105–20.

16. Zhang J, Li S, Li L, Li M, Guo C, Yao J, Mi S. Exosome and exosomal microRNA: trafficking, sorting, and function. Genomics Proteomics Bioinformatics. 2015;13(1):17–24.
17. Qiu G, Zheng G, Ge M, Wang J, Huang R, Shu Q, Xu J. Mesenchymal stem cell-derived extracellular vesicles affect disease outcomes via transfer of microRNAs. Stem Cell Res Ther. 2018;9(1):320.
18. Gheinani AH, Vogeli M, Baumgartner U, Vassella E, Draeger A, Burkhard FC, Monastyrskaya K. Improved isolation strategies to increase the yield and purity of human urinary exosomes for biomarker discovery. Sci Rep. 2018;8(1):3945.
19. Lv LL, Wu WJ, Feng Y, Li ZL, Tang TT, Liu BC. Therapeutic application of extracellular vesicles in kidney disease: promises and challenges. J Cell Mol Med. 2018;22(2):728–37.
20. Guan H, Peng R, Mao L, Fang F, Xu B, Chen M. Injured tubular epithelial cells activate fibroblasts to promote kidney fibrosis through miR-150-containing exosomes. Exp Cell Res. 2020;392(2):112007.
21. Pan T, Jia P, Chen N, Fang Y, Liang Y, Guo M, Ding X. Delayed Remote Ischemic Preconditioning ConfersRenoprotection against Septic Acute Kidney Injury via Exosomal miR-21. Theranostics. 2019;9(2):405–23.
22. Meng XM, Ren GL, Gao L, Yang Q, Li HD, Wu WF, Huang C, Zhang L, Lv XW, Li J. NADPH oxidase 4 promotes cisplatin-induced acute kidney injury via ROS-mediated programmed cell death and inflammation. Lab Invest. 2018;98(1):63–78.
23. Zhang R, Yin L, Zhang B, Shi H, Sun Y, Ji C, Chen J, Wu P, Zhang L, Xu W, Qian H. Resveratrol improves human umbilical cord-derived mesenchymal stem cells repair for cisplatin-induced acute kidney injury. Cell Death Dis. 2018;9(10):965.
24. Wu M, Wang Y, Yang D, Gong Y, Rao F, Liu R, Danna Y, Li J, Fan J, Chen J, Zhang W, Zhan Q. A PLK1 kinase inhibitor enhances the chemosensitivity of cisplatin by inducing pyroptosis in oesophageal squamous cell carcinoma. EBioMedicine. 2019;41:244–55.
25. Li ZL, Lv LL, Tang TT, Wang B, Feng Y, Zhou LT, Cao JY, Tang RN, Wu M, Liu H, Crowley SD, Liu BC. HIF-1alpha inducing exosomal microRNA-23a expression mediates the cross-talk between tubular epithelial cells and macrophages in tubulointerstitial inflammation. Kidney Int. 2019;95(2):388–404.
26. Bao H, Zhang Q, Liu X, Song Y, Li X, Wang Z, Li C, Peng A, Gong R. Lithium targeting of AMPK protects against cisplatin-induced acute kidney injury by enhancing autophagy in renal proximal tubular epithelial cells. FASEB J. 2019;33(12):14370–81.
27. Ho J, Kreidberg JA. The long and short of microRNAs in the kidney. J Am Soc Nephrol. 2012;23(3):400–4.
28. Lee CG, Kim JG, Kim HJ, Kwon HK, Cho IJ, Choi DW, Lee WH, Kim WD, Hwang SJ, Choi S, Kim SG. Discovery of an integrative network of microRNAs and transcriptomics changes for acute kidney injury. Kidney Int. 2014;86(5):943–53.
29. Yang Y, Li HY, Zhou Q, Peng ZW, An X, Li W, Xiong LP, Yu XQ, Jiang WQ, Mao HP. Renal Function and All-Cause Mortality Risk Among Cancer Patients. Medicine. 2016;95(20):e3728.

30. Linkermann A, Chen G, Dong G, Kunzendorf U, Krautwald S, Dong Z. Regulated cell death in AKI. J Am Soc Nephrol. 2014;25(12):2689–701.
31. Tonnus W, Gembardt F, Latk M, Parmentier S, Hugo C, Bornstein SR, Linkermann A. The clinical relevance of necroinflammation-highlighting the importance of acute kidney injury and the adrenal glands. Cell Death Differ. 2019;26(1):68–82.
32. Barile L, Vassalli G. Exosomes: Therapy delivery tools and biomarkers of diseases. Pharmacol Ther. 2017;174:63–78.
33. Zhang W, Zhou X, Zhang H, Yao Q, Liu Y, Dong Z. Extracellular vesicles in diagnosis and therapy of kidney diseases. Am J Physiol Renal Physiol. 2016;311(5):F844–51.
34. Zhu G, Pei L, Lin F, Yin H, Li X, He W, Liu N, Gou X. Exosomes from human-bone-marrow-derived mesenchymal stem cells protect against renal ischemia/reperfusion injury via transferring miR-199a-3p. J Cell Physiol. 2019;234(12):23736–49.
35. Lv LL, Feng Y, Wu M, Wang B, Li ZL, Zhong X, Wu WJ, Chen J, Ni HF, Tang TT, Tang RN, Lan HY, Liu BC. Exosomal miRNA-19b-3p of tubular epithelial cells promotes M1 macrophage activation in kidney injury. Cell Death Differ. 2020;27(1):210–26.
36. Cheng Q, Wang L. LncRNA XIST serves as a ceRNA to regulate the expression of ASF1A, BRWD1M, and PFKFB2 in kidney transplant acute kidney injury via sponging hsa-miR-212-3p and hsa-miR-122-5p. Cell Cycle. 2020;19(3):290–9.
37. Li X, Zeng L, Cao C, Lu C, Lian W, Han J, Zhang X, Zhang J, Tang T, Li M. Long noncoding RNA MALAT1 regulates renal tubular epithelial pyroptosis by modulated miR-23c targeting of ELAVL1 in diabetic nephropathy. Exp Cell Res. 2017;350(2):327–35.

Figures

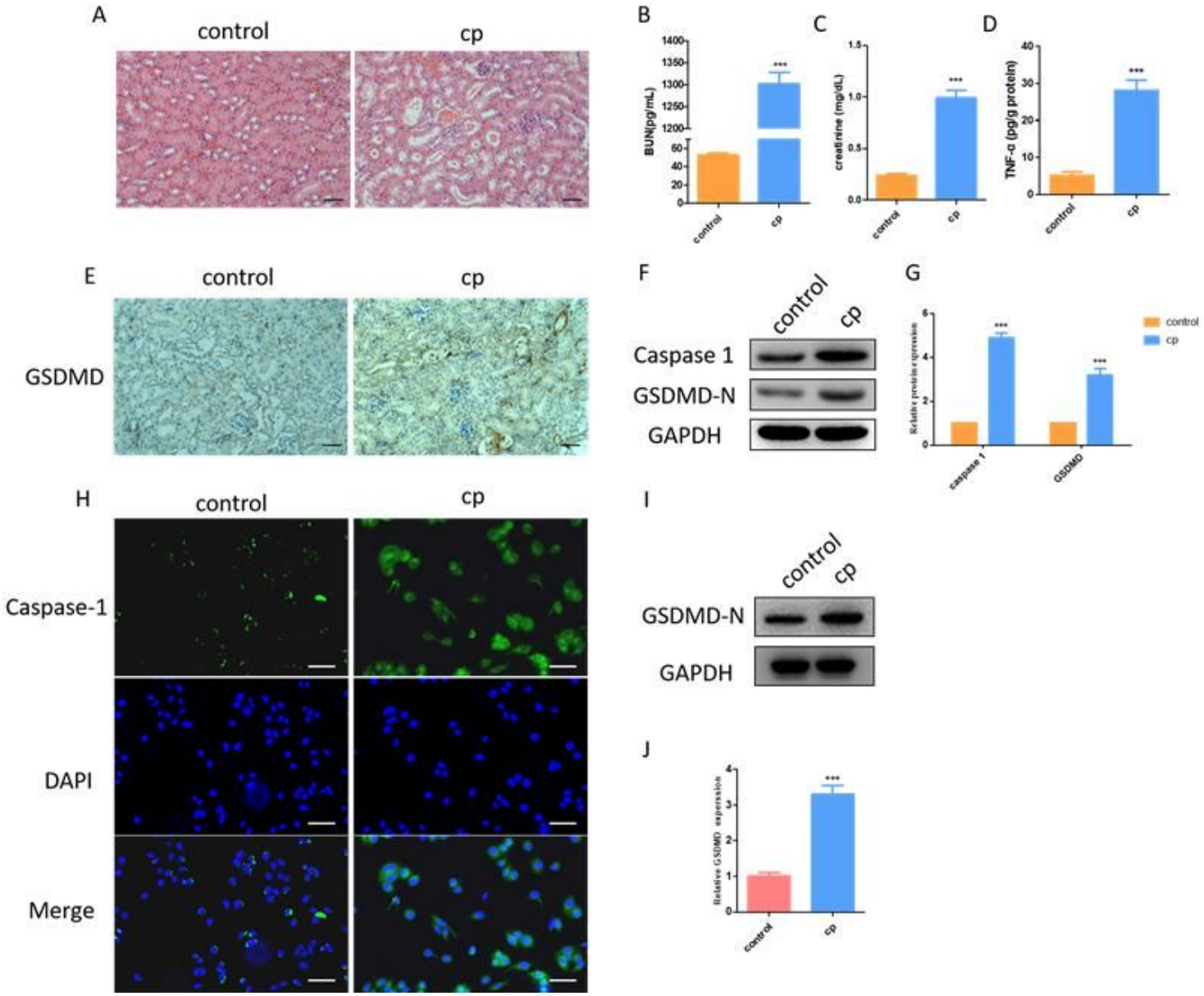

Figure 1

Cisplatin induces mouse AKI and RTECs pyroptosis. (A) H&E staining assays were performed 24 h after surgery in both cisplatin-induced AKI mouse model group and control group. (B) - (D) After AKI was induced by cisplatin treatment, blood was sampled for BUN, serum creatinine and TNF-α concentration. (E) The distribution of GSDMD in kidney tissues measured by IHC. (F) - (G) WB analysis of caspase-1 and GSDMD-N expression in cisplatin-induced AKI mice. (H) IF staining showed expression of caspase-1 (green) in cisplatin-treated HK2 cells; Blue fluorescence represents the nucleus (DAPI). Bar, 100 mm. (I) - (J) WB analysis of caspase-1 and GSDMD-N expression in cisplatin-treated HK2 cells. Data are shown as mean ± SEM (n=3). Asterisks indicate significant differences from the control (*, $p < 0.05$; **, $p < 0.01$; ***, $p < 0.001$).

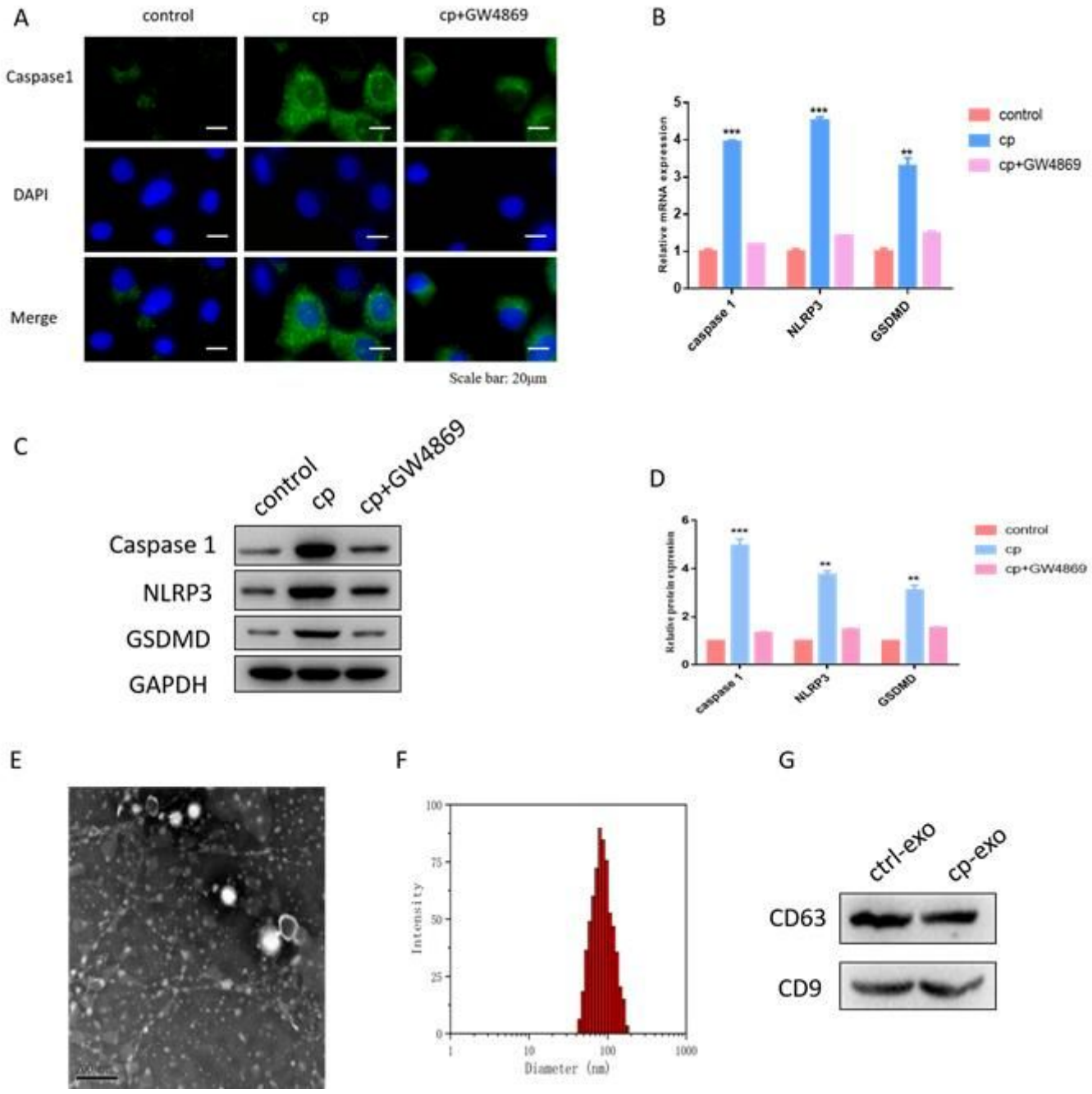

Figure 2

HK2 cell-derived exosomes treated with cisplatin influenced pyroptosis of surrounding HK2 cells. (A) IF staining showed expression of caspase-1 (green) in cisplatin-treated and cisplatin+ GW4869-treated HK2 cells, respectively; Blue fluorescence represents the nucleus (DAPI). Bar, 20 mm. (B) The qPCR analysis of caspase-1, NLRP3 and GSDMD expression in cisplatin-treated and cisplatin+GW4869-treated HK2 cells. (C) - (D) WB analysis of caspase-1, NLRP3 and GSDMD expression in cisplatin-treated and cisplatin+GW4869-treated HK2 cells. (E) The transmission electron microscope (TEM) image of exosomes isolated from HK2 cells, revealing the typical morphology and size (30 and 150 nm). (scale bar, 200 nm). (F) The particle diameter (nm) of the population of small vesicles collected from HK2 cells were detected using qNano. (G) WB showed that exosome marker CD63 and CD9 were expressed in exosomes.

Data are shown as mean ± SEM (n=3). Asterisks indicate significant differences from the control (*, p < 0.05; **, p < 0.01; ***, p < 0.001).

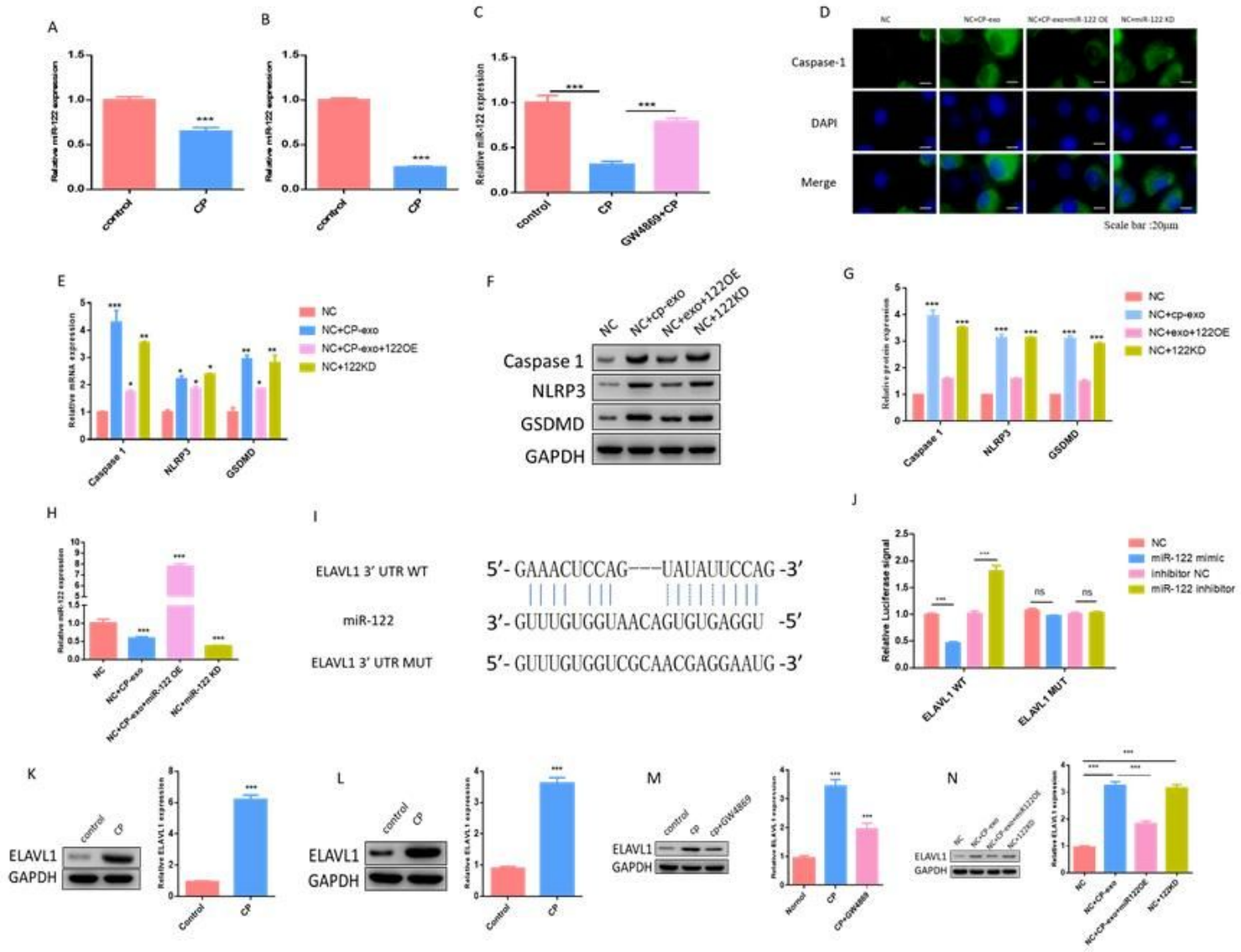

Figure 3

Cisplatin-treated HK2 cells exosome-derived miR-122 regulates pyroptosis in surrounding cells. (A) – (B) The qPCR analysis of miR-122 expression in vivo and in vitro when adding cisplatin treatment. (C) The qPCR analysis of miR-122 expression. (D) IF staining showed expression of caspase-1 (green); Blue fluorescence represents the nucleus (DAPI). Bar, 20 mm. (E) The qPCR analysis of caspase-1, NLRP3 and GSDMD expression. (F) - (G) WB analysis of caspase-1, NLRP3 and GSDMD expression. (H) The qPCR analysis of miR-122 expression. (I) 3'-UTR base pairing diagram of miR-122 and ELAVL1. (J) Cells were co-transfected with miR-122 mimics/inhibitor and a luciferase reporter containing a fragment of the ELAVL1 3'-UTR harboring either the miR-122 binding site (ELAVL1-3'-UTR-WT) or a mutant (ELAVL1-3'-UTR-MUT). (K)-(N) The protein expression of ELAVL1 in vivo and in vitro under different processing conditions. Data are shown as mean ± SEM (n=3). Asterisks indicate significant differences from the control (*, p < 0.05; **, p < 0.01; ***, p < 0.001).

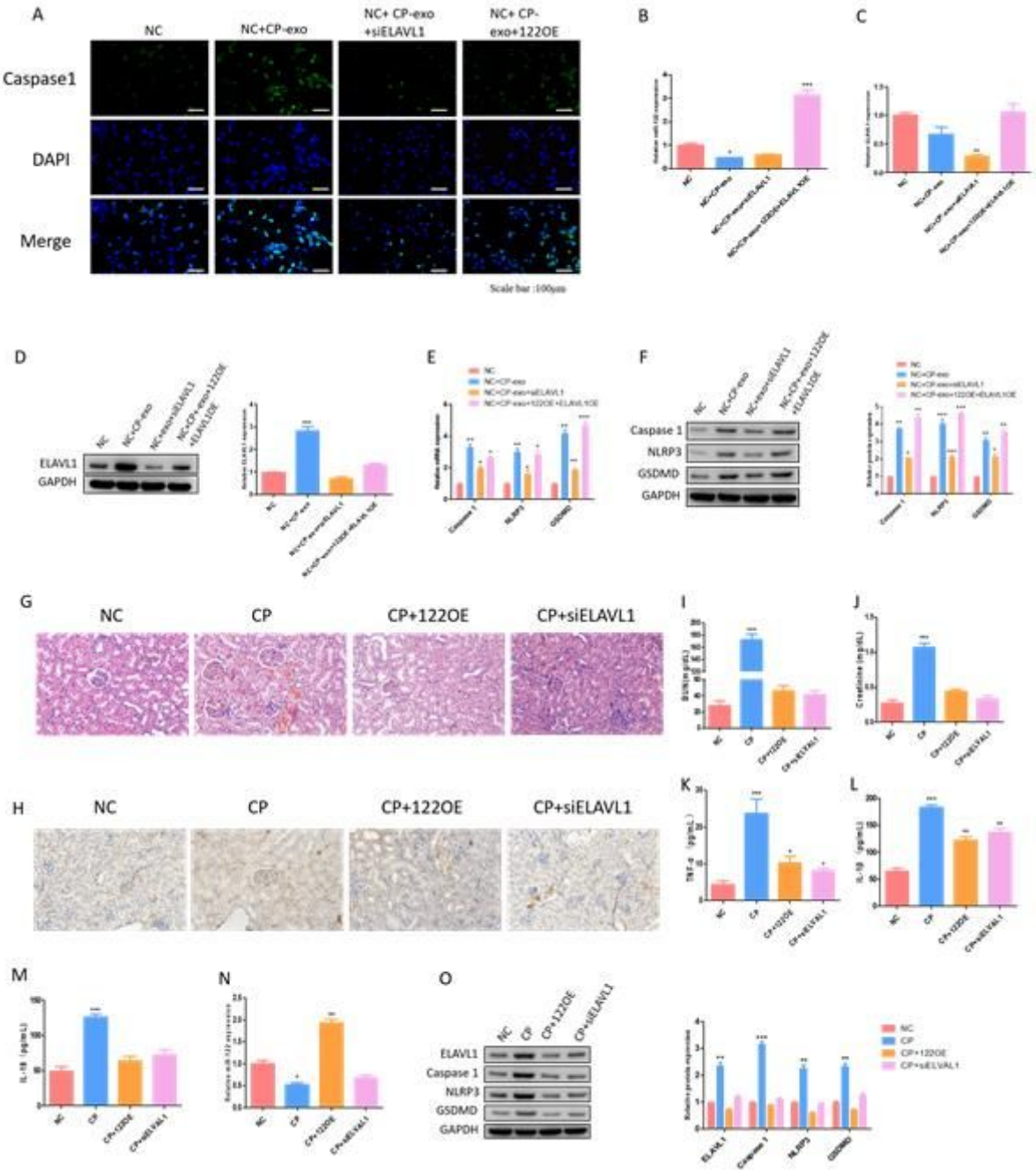

Figure 4

Exosome-derived miR-122 affects cisplatin-induced AKI and HK2 cells pyroptosis by regulating the expression of ELAVL1. (A) IF staining showed expression of caspase-1 (green); Blue fluorescence represents the nucleus (DAPI). Bar, 100 mm. (B) - (C) The qPCR analysis of miR-122 and ELAVL1 expression. (D) WB analysis of ELAVL1 expression. (E) The qPCR analysis of caspase-1, NLRP3 and GSDMD expression. (F) WB analysis of caspase-1, NLRP3 and GSDMD expression. (G) H&E staining assays. (H) The distribution of GSDMD in kidney tissues measured by IHC. (I) – (M) The blood came from AKI mice was sampled for BUN, serum creatinine, TNF-α, IL-1β and IL-18 concentration. (N) The qPCR analysis of miR-122 expression. (O) The WB analysis of ELAVL1, caspase-1, NLRP3 and GSDMD

expression. Data are shown as mean ± SEM (n=3). Asterisks indicate significant differences from the control (*, $p < 0.05$; **, $p < 0.01$; ***, $p < 0.001$).